Advances in Science and Technology Research Journal

Advances in Science and Technology Research Journal 2024, 18(5), 90–100
https://doi.org/10.12913/22998624/190128
ISSN 2299-8624, License CC-BY 4.0

Received: 2024.05.10
Accepted: 2024.06.25
Published: 2024.08.01

Characteristics of the Porous Structure Developed Through Additive Manufacturing Using Polyamide for Tissue Engineering Applications

Szymon Sikora[1], Ewa Bednarczyk[1*], Roman Grygoruk[1], Mariusz Fabijański[2], Andrzej Aniszewicz[3]

[1] Faculty of Mechanical and Industrial Engineering, Department of Machine Construction and Biomedical Engineering, Warsaw University of Technology, ul. Narbutta 85, 02-524, Warsaw, Poland

[2] Faculty of Mechanical and Industrial Engineering, Plastics Processing Department, Warsaw University of Technology, ul. Narbutta 85, 02-524, Warsaw, Poland

[3] Railway Institute, Metrology Laboratory, ul. Chłopickiego Józefa 50, 04-275 Warsaw, Poland

* Corresponding author's e-mail: ewa.bednarczyk@pw.edu.pl

ABSTRACT

Additive manufacturing methods give the opportunity to produce interesting, new structures with a more complicated topology than would be possible using traditional methods. Using the selective laser sintering method, a disk with a high roughness and porous structure was produced. Studies of material surface were performed on microscopic devices. An in vitro experiment was performed on the manufactured disk using mice fibroblastic cells. The designed shape enabled the growth of the cell culture in the disc pores and ensured impermeability of the disc base. On the basis of the average viability of 79%, which is close to reference well (80%), preliminary results confirmed that the manufactured structures create sufficiently comfortable conditions for the cell cultures without the need to design their internal topography. Controlling the production parameters of SLS printing allows obtaining the structures characterized by spatial and surface porosity without designing inner geometry of the structure. Polyamide 2200 (PA2200) powder with a laser beam, offers new possibilities for producing surfaces used in the tissue engineering, bioreactors, and microfluidics devices.

Keywords: 3D printing, cell culture, SLS method, biomechanical engineering.

INTRODUCTION

The phenomenon called tissue engineering has been known since the early 1980s. It was a response to the challenges associated with research on bacteria, cells, implantology and transplantology. It combines knowledge from various areas of science, including biology, genetics, biochemistry, chemistry, medicine, materials engineering, and technology. One of the primary goals of tissue engineering is to develop three-dimensional, porous structures called scaffolds, which are intended to provide an appropriate environment for the regeneration of damaged tissues or organs and are utilized in in-vitro research. These scaffolds are intended to simulate extracellular matrix (ECM) and should be identical or like that found in living organisms, providing support for cells, and regulating regenerative processes. After preparation of in vitro exploration, e.g. in bioreactors, tissue substitutes can be implanted in the place of damaged tissue or organ, where they continue the regeneration process in vivo [1]. ECM has to perform a lot of features, both at the cellular, tissue and organ levels. The appropriate design of the scaffold and adapting its properties to specific needs is a significant issue so as to deliver the tissue to the defect site as well as provide an appropriate environment for the reconstruction of a given tissue [2, 3].

The use of 3D additive manufacturing technology for the production of lab-on-a-chip systems is

not a widespread [4] and is still under development. A dynamic advance of this relatively new production technology opens up new fields for its use [5, 6]. An increase of number of publications has demonstrated the usefulness of 3D printing as a method for manufacturing microbioreactors [7, 8, 9, 10]. This method is characterized by a high ability to create complex structures precisely and automatically on a small scale. 3D printing enables manufacturing micro-bioreactors with complex shapes and structures, which is crucial for ensuring optimal environmental conditions for cell cultures or microorganisms. Additionally, the ability for rapid prototyping and customization of designs to specific needs makes this technology an attractive option in the production of structures and cultivation bioreactors.

It is worth noting that the use of 3D printing in the production of micro-bioreactors may contribute to the development of other new technologies in the field of biotechnology, enabling more precise experiments and the production of small batches of drugs or biological substances.

Furthermore, this technology brings about numerous advantages, such as reduction of the production costs [11], simplified course of some methodologies [12] (FDM, lamination, SL), and also allows for designing empty spaces inside the material, which is practically impossible with standard production methods. Currently, commercial 3D printing devices already offer printing resolution of 1–200 μm and may use biocompatible materials. This spikes a growing interest in the use of these methods in the production of systems utilized in tissue engineering, such as micro bioreactors [13, 14, 15].

In this work, one of the 3D printing technologies called SLS (Selective Laser Sintering) was used to produce porous structures [16, 17, 18]. It is one of the fundamental methods of rapid prototyping, belonging to the group of Powder Bed technologies, characterized by the selective bonding of successive layers of powder from a given polymeric material. In the method, a laser fuses particles of powdered thermoplastic material, joining them into successive layers. The SLS technology finds wide application, both in prototyping and in small-scale production of functional parts made of plastics with good mechanical properties. Currently, among all available 3D printing technologies, it is the most commonly used method in small-scale production of final parts of machines and technical devices [19, 20, 21]. An undeniable advantage of this technology is the great freedom in design, high accuracy of produced elements, and production of parts with mechanical properties comparable to the properties of elements manufactured conventionally. It also offers possibilities for producing complex porous structures [22, 23, 24, 25, 26].

The material most often used in this technology is polyamide. These materials constitute a whole family of different varieties intended mainly for machine construction due to their good mechanical properties. Polyamides are also characterized by moisture absorption. From the point of view of processing methods and use, this is an unfavorable feature. However, in the case under consideration, moisture absorption is an added value. In the SLS technology, it is used in the form of powder. Polyamides are characterized by good temperature resistance and biocompatibility [27].

The aim of the undertaken research was the motivation and necessity to develop a certain type of quasi-spatial and porous structure for cell culture. Such designs could be used in the future for designing and producing bioreactors and lab-on-a-chip systems for more advanced research. The main characteristic feature of the proposed design, compared to existing ones, is the random nature of the spatial porosity arrangement. As literature states, a spatial porous structure is designed at the stage of preparing a virtual model, where obtaining a real substrate later may not be achievable. In the considered solution, it should therefore be acknowledged that the proposed method of creating the structure seems more realistic and may be suitable for cell culture [26, 28, 29, 30, 31].

MATERIALS AND METHODOLOGY

Materials

The PA 2200 polyamide from EOS HmbH Electro Optical Systems company was used in the research [32, 33, 34]. This is a powder intended for use in all SLS printing systems. The recommended layer thickness is 0.1 mm. Unfused powder can be reused. The material properties and its form ensure consistent process parameters and simultaneously guarantee the production of high-quality products. The study did not account for variations in the powder grain size. The material was utilized in its commercial form without any additional modifications. The process,

when applied to the same material under identical technological parameters, is fully repeatable. The consistency and repeatability of the process parameters ensure that there are no changes in surface roughness. It can also be used for fully functional prototypes that easily withstand high mechanical and thermal loads [35, 36]. Table 1 provides the basic properties of the material.

Models made from PA 2200 are characterized by chemical resistance, significant strength, and stability of material degradation over time. They are also described as highly versatile, not only in industry but also in medicine. In terms of mechanical strength and flexibility, products made from polyamide 2200 are compared to items produced by injection molding [37, 38, 39].

Samples manufacture

To prepare samples for surface topography research, a FORMIGA P100 3D printer from EOS HmbH Electro Optical Systems was used. This is a comprehensive three-dimensional printing system utilizing Selective Laser Sintering (SLS) technology. It allows for obtaining extremely precise, accurate, and fully functional models from polymer materials in a short time based on 3D CAD files. The device allows for selecting (optimizing) the appropriate parameters of the laser beam to melt or sinter particles of powder in precisely defined areas.

Model preparation

The model in the form of a disk, which serves as the scaffold (Figure 1a and 1b) for the cell culture base surface, was previously prepared using Solid Works 3D software. It was then produced by sintering the grains of the batch material and its diffusive bonding, which enabled obtaining the desired porous structure using SLS technology [40]. The whole process starts with a 3D model, which is input into the machine's memory. After selecting the parameters of the technological process, the printing process is initiated according to the scheme presented in Figure 2.

Table 1. Features of PA2200

Material parameters (powder)		
Grain size distribution	µm	38.8–88.3
Unsintered powder density	g/cm^3	0.435–0.445
Sintered powder density	g/cm^3	0.9–0.95
Mechanical properties		
Tensile strength	MPa	45 ± 3
Elongation at break	%	50 ± 5
Charpy impact strength	kJ/m^2	53 ± 3.8
Ball hardness	MPa	77.6 ± 2
Thermal properties		
Melting temperature	°C	172–180
Softening temperature according to Vicat A/50	°C	181
Softening temperature according to Vicat B/50	°C	163

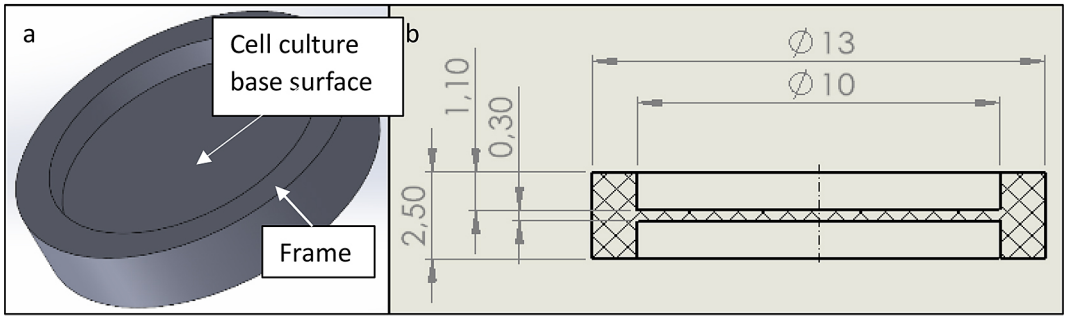

Figure 1. Culture disc: (a) 3D model of a structure suggested for use in tissue engineering, (b) dimensions of the culture disc

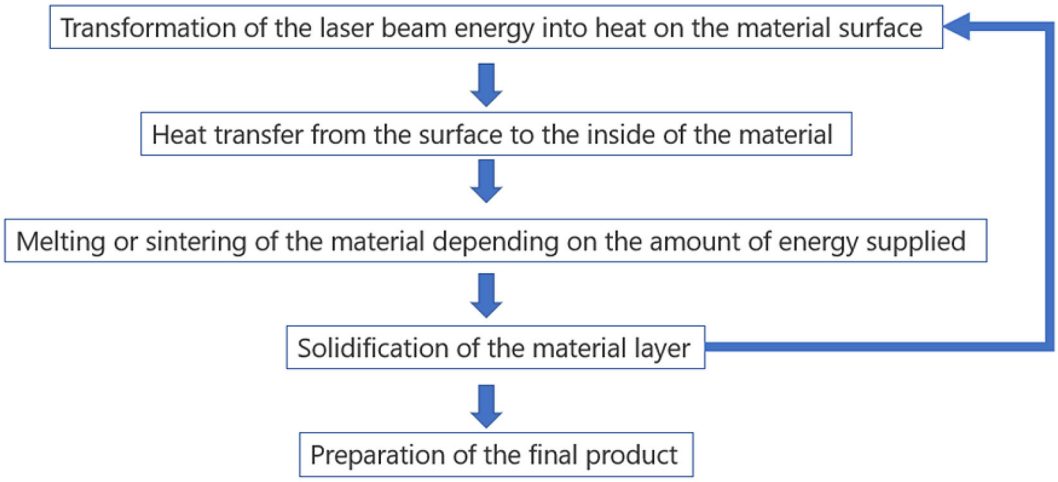

Figure 2. Diagram of a product manufacturing with SLS method

During the process, the machine bed is filled with a layer of powder of a specific degree of fineness and grain shape, which is then spread to achieve a uniform layer. The spread material is sintered along programmed paths where the laser beam moves, solidifying the designed shape. The thickness of the solidified paths depends on several factors, such as machine accuracy, laser power, powder morphology, and programmed layer height. After sintering a given layer, the printer bed was replenished with powder, and the entire process was repeated for the next layer [19, 20]. Importantly, it should be emphasized that the layers can be permeable, impermeable, or partially permeable. In the considered case, a porous structure was desired. Therefore, it was necessary to choose appropriate laser parameters, which determine the degree of material sintering. The process parameters assumed the laser energy of 16 W at a beam sweep speed of 3000 mm/s. The temperature of the material in the layer space was 175 °C with the powder bed temperature of 154 °C. The printing resolution in the model increment axis was 0.1 mm. Such selection of process parameters enabled the creation of a stochastic structure; consequently, each sample prepared for testing had its unique surface structure and pore distribution. These characteristics were derived from the combination of the model design, its modifications, and the material properties of the polyamide used.

The bottom layer of the cell culture base structure was sintered twice to ensure impermeability of the layer, while the next 3 layers were sintered in a single pass of the laser, thereby creating a spatially porous structure. Process parameters were adjusted so that in the upper layers of the cell culture base structure, material particles were not completely melted, but only partially melted on their surface to a degree sufficient to bond with adjacent powder grains, thus forming a permeable spatially porous structure.

Due to the random arrangement of PA2200 grains in each layer, there was no need to design a repeatable porous structure at the CAD geometric modeling stage.

In vitro tests

The study utilized the WEHI 164 mouse Cell Line (Sigma-Aldrich® Solutions), obtained from the manufacturer from fibrosarcoma. The cells grow to sizes of 20 µm and are relatively uncomplicated to incubate. Figure 3 shows an example of the fibroblast culture used in the study after approximately a week of cultivation in the E. J. Brzeziński Biomedical Engineering Laboratory.

During the experiment, the WEHI 164 cells were grown in MegaCell™ RPMI-1640 base medium enriched with 2 mM glutamine and 10% fetal bovine serum (FBS). The dimensions of the culture discs were adjusted to the dimensions of the wells on the NUNC cell culture plates, so that they fit easily. The frame of the culture disc protected the cells from flowing down from the culture surface into the well. The cell seeding was divided into two steps. The first step was to administer 50 µl of RPMI 1640 culture medium with the WHI164 cell line to the culture disc. Then, after 4 h incubation in the Thermo Fisher Scientific Steri-Cycle i160 incubator at 37 °C and in the presence of 5% CO_2, 250 µl of the prepared cell culture medium were added to each well.

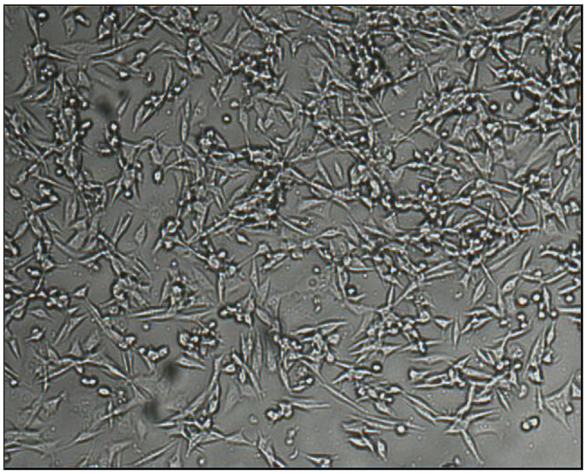

Figure 3. An illustrative image of a monolayer culture of mouse fibroblasts obtained on the NanoEntek Digital Bio JuLI FL smart fluorescent cell analyzer

In order to prepare the porous material for the cell culture, the disc was mechanically cleaned after printing in accordance with the manufacturer's recommendations, while maintaining appropriate purity standards. Then, the residue of the powder grains and the surface-unbound melting of the grains were removed during ultrasonic washing (2 × 20 minutes) in the EMAG EMMI 4 ultrasonic cleaner. The cleaned base model was then sterilized by repeated rinsing with 70% ethanol and autoclaved in NUVE NC 40M vertical autoclave at 137 °C for 20 minutes. After that, it was transferred to the Thermo Fisher Scientific MSC ADVANTAGE 1.2 laminar flow hood, and immersed again in 70% ethanol for 30 minutes. After drying, the prints were exposed to UV light. The prepared structure was placed in a 24 – well plate (SPL Life Sciences) (Figure 4).

Five culture disks underwent biocompatibility tests. They were placed in wells A2 to A6, and the A1 well was designated as the reference well, with a nonporous surface, typical commercial culture vessel (manufactured by for example SPL Life Science).

The cell suspension (50 µl, 10^4 cells/ml) was applied to the surfaces of the disks and the reference well, and the cultures were incubated for approximately 4 hours in an incubator. After this time, 250 µl of culture medium was poured into each well, and they were left for further incubation. The medium was exchanged every 2 days. Microscopic observations were conducted after one week of culture incubation.

To determine the cell count and the ratio of live cells to the total population in the well – the viability of the culture, a NanoEntek EVE automatic cell counter was used. The cells were subjected to trypsinization, a process involving the removal of the medium from the culture vessel and its replacement with a trypsin solution. Firstly, 1.5 ml of trypsin solution was added to each well to cover the entire culture surface, and then the culture was placed in an incubator for 15 minutes to activate trypsin action at every possible location in the structure. A 15 – minute duration was safe for the cells and ensured complete detachment of the cells from the surface of the structures in

Figure 4. Cell culture in a 24 – well plate. Culture discs prepared for incubation

the reference well. The cell suspension was transferred to a 15 ml Falcon tube and centrifuged in an AFI MULTILAB CENTRIFUGES 0.6 L Siren centrifuge at 3000 rpm for 3 minutes, which allowed the cells to settle at the bottom of the tube. After centrifugation, the supernatant above the cells was removed and replaced with fresh medium to a volume of 3 ml. Meanwhile, tubes with a capacity of containing 20 µl of warmed trypan blue were prepared. The fresh cell suspension was pipetted to ensure even distribution of cells throughout the liquid volume. Homogeneous cell suspension was added to the trypan blue at a volume of 20 µl and incubated at 37 °C for 3 minutes. After 3 minutes, the suspension with stained cells was placed in counting chambers at a volume of 10 µl per chamber, and cell viability testing was conducted. The viability test results are presented in Table 2, showing the percentage of live, unstained cells out of all counted cells. On the basis of this test, it was determined whether the produced quasi-porous structure can be used as a cultivation substrate for the WEHI 164 cells and how it affects their viability and proliferation.

To measure surface roughness, a Keyence VHX 950F digital microscope with a Keyence VH-Z100R lens was used, allowing observations with magnifications ranging from x100 to x1000, along with dedicated software provided by the manufacturer. This software enables the measurement of various parameters, including surface roughness, the creation of a three-dimensional surface model, and volumetric analysis. The roughness measurement was conducted based on a sequence of captured images of the tested structure taken at different lens heights. The lens step, and therefore the difference in the recorded plane, was 0.2 µm. Subsequently, based on the captured images, the software processed the data to create a three-dimensional surface model (Figure 5) and allowed for further analysis regarding surface roughness.

The conducted roughness measurement is a non-contact method that utilizes light interference to determine the distance of an object from the lens. The microscope software compares the reference distance that the light beam should travel with the distance traveled by the beam reflected from the object. After processing the data collected from the measurements, the surface roughness parameter Sa can be obtained. The advantage of this measurement method is the short time required to perform the measurements, a wide range of surface parameters that can be determined based on a single recorded image series, and ease of measurement compared to commonly used profilometers, due to the lack of necessity to select the appropriate tool size for the measured size.

Using the software provided by the manufacturer, a series of parameters describing surface roughness was determined. Below is a list of the examined parameters along with their brief descriptions:

- Sa – arithmetical mean height – average or arithmetic average of the profile height deviations from the mean surface,
- Sz – maximum height – sum of the largest peak height value and the largest pit depth value within the definition area,
- Sq – root means square height – value of ordinate values within the definition area,
- Ssk – skewness – value representing the degree of bias of the roughness shape (asperity),
- Sku – kurtosis – value representing the measure of the sharpness of the roughness profile,
- Sp – maximum peak height – height of the highest peak within the definition area,
- Sv – maximum pit height – the absolute value of the height of the largest pit within the definition area.

RESULTS

The assumptions regarding the geometry and shape parameters of the model, combined with the 3D printing parameters and the batch material PSD at a level of 56 µm, resulted in the creation of a model with roughness ranging from 60–100 µm. On the basis of the assumptions and previously acquired knowledge, it was determined that the obtained parameters of the structure are optimal for conducting WEHI 164 cell cultures. The print made using SLS technology with PA2200 powder allowed for the creation of a structure characterized

Table 2. Cell viability in wells

Well	A1	A2	A3	A4	A5	A6
Viability	80%	76%	77%	81%	82%	79%

by both spatial and surface porosity. The porosity of the model was intended to enhance the development of WEHI 164 mouse fibroblast cultures and enable the creation of quasi-spatial cultures. To verify the surface and spatial parameters of the produced structure, images taken with a Keyence VHX-950F digital microscope were used, which were then analyzed using the software provided with the microscope (Figure 5b, 5c).

The specific geometry of the model allowed for the limitation of the surface area where the cell culture was conducted solely to the produced cultivation disk (Figure 5a). The designed frame enabled the pouring of a cell suspension in a volume of 50 µl only onto the surface of the produced structure and prevented the cells from flowing beyond the desired area.

The obtained cell culture base surface disks were characterized by a roughness (Sa) at the level of 11.65 µm (Table 3), and the pore size reached up to 100 µm with an average of 37.5 µm (Figure 6). In Table 3, the surface parameters of the disks obtained from the analysis of images taken with a Keyence VHX 950F digital microscope were presented.

Due to the preliminary nature of the presented research and the necessity to verify process parameters and material selection, the assessment of the structure influence on the culture was limited to monitoring changes in the color of the medium and conducting a viability test. The color of the cultivation medium changed uniformly in each well, both with the examined structures and in the reference well (Figure 7a, 7b). A color change from pink to yellow - orange was observed every other day after medium exchange, indicating growth of the culture and consumption of nutrients from the medium. It was impossible to extract all cells populated in the structures without damaging the structures or cells (trypsin exposure time without its negative impact). Cells were detached from the substrate using a standard trypsinization protocol. Cells were immersed in trypsin and incubated for 2 minutes, then, after decanting the trypsin, they were incubated for an additional 5 minutes. The trypsinization results are shown in (Figure 7d), where approximately 1/3 of the cells were flushed out from the cultivation disks.

On the basis of the observation of the medium color and its comparison between the reference well and the wells with the placed cultivation disks, it was possible to exclude a negative impact of the disks on the development of tissue culture. To support this observation, a viability test was performed using trypan blue. The test results showing similar viability of all cultures are presented in Table 2.

DISCUSSION

The use of SLS technology allowed achieving the desired porosity of the produced structures.

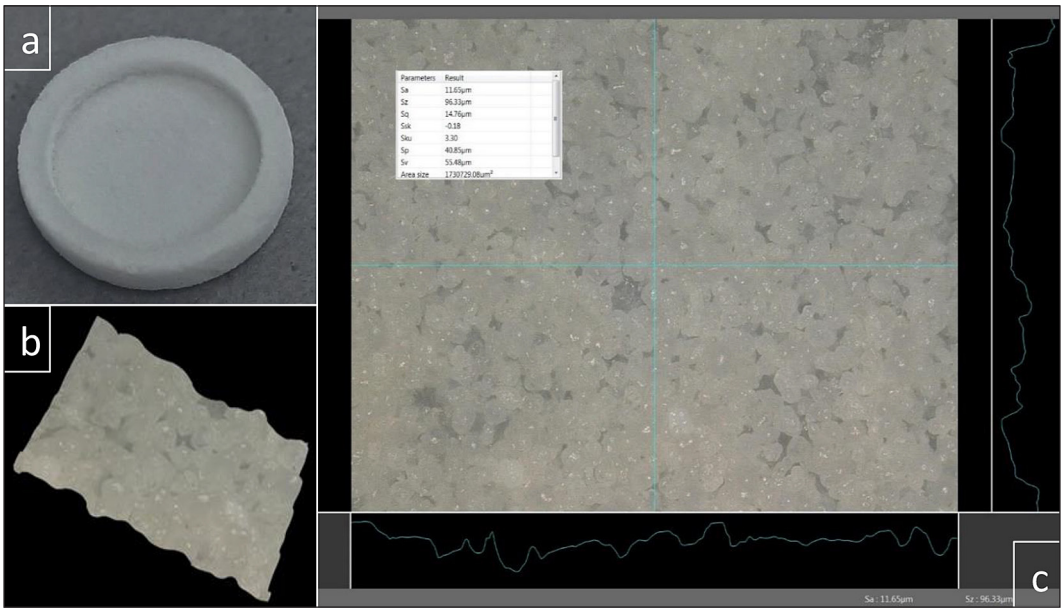

Figure 5. (a) photo of the printed culture disc, (b) 3D model of the structure based on the micrographs taken at a 500× magnification, obtained with the software included with the Keyence VHX 750 microscope, (c) surface roughness analysis

Table 3. Parameters characterizing the obtained surface structure. The micrographs were captured at a 500× magnification and then analyzed using the Keyence VHX 750 microscope

Parameter	Value
S_a	11.65 µm
S_z	96.33 µm
S_q	14.76 µm
S_{sk}	-0.18
S_{ku}	3.30
S_p	40.85 µm
S_v	55.48 µm
Area size	1730729.08 µm^2

The designed shape of the structure enabled cell culturing only in the area of the cell culture bad surface disk. The authors' previous experiences suggested the need to create a structure that would allow limiting the culture surface to a strictly controlled area, which is particularly important during the initial phase of setting up the culture. In the beginning, structures with a flat surface were tested, which significantly hindered the proper initiation of the culture and its limitation only to the investigated surface. The geometry of the produced disk facilitated the colonization of the structure by cells, and the disk frame prevented the cell suspension from spilling beyond the porous structure.

To separate the cells from the structure, trypsinization was conducted. For research purposes, the trypsinization time was extended to the longest possible duration that was safe for the cells, which was 2 minutes. As a result of trypsinization, approximately 1/3 of the expected number of cells exited the pores of the disk (Figure 7d). This likely resulted from cells occupying pores from which it was difficult or impossible to extract despite rinsing the structure. Staining live cells within the pores of the structure should confirm the assumptions about the "comfort" of the structure for the cells. For such staining, MTT [3-(4,5-dimethylthiazol-2-yl)-2,5-diphenyltetrazolium bromide] can be utilized [21, 22]. Nevertheless, observing the color change of the medium before and after trypsinization is sufficient to confirm the usefulness of employing SLS technology for producing in vitro systems and cell culture substrates. However, it is important to consider the limitations associated with this

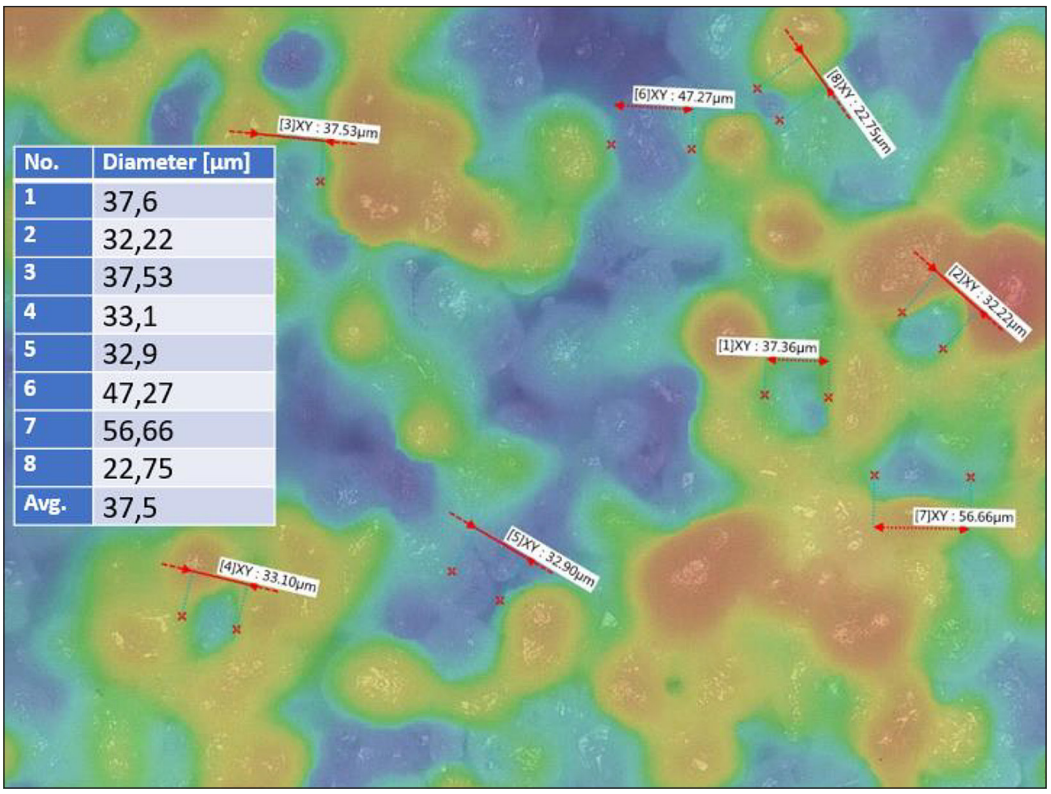

Figure 6. Analysis of the surface structure with marked size of sample pores. The analysis was carried out on images captured at a 500× magnification using the software included with the Keyence VHX 750 microscope

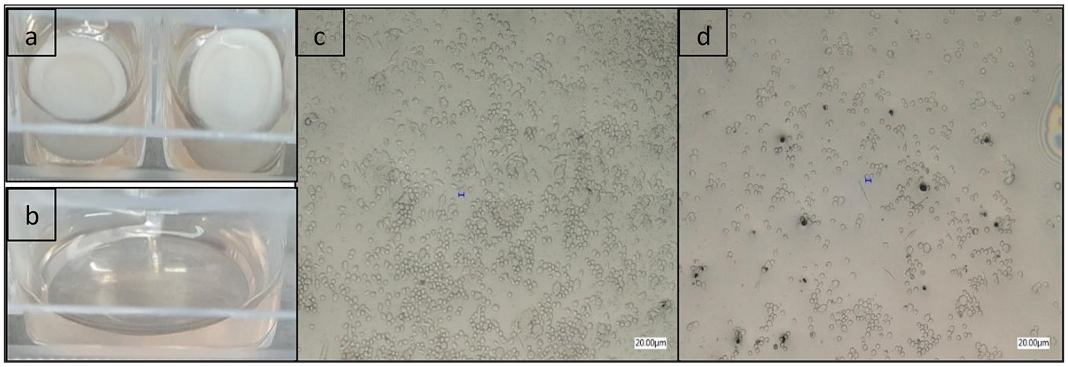

Figure 7. (a) samples in wells A2 and A3, (b) reference well, (c) reference well, magnification 200×, (d) detached cells in the A4 well with dead cells stained in dark blue, magnification 200×

technology. One of the more significant limitations is the ability to use only batch materials that absorb the laser beams light, which translates to the inability to use transparent materials. These materials are desired for observing cell cultures, but this limitation does not make it impossible. To mitigate this constraint, a 3D printer using SLS technology should be equipped with a laser of a wavelength outside the visible light range, e.g., a CO_2 laser [41]. Unfortunately, due to the sintering of transparent powder, a transparent structure cannot be obtained. This limitation necessitates the use of reflected/incident light microscopes, rather than transmitted light microscopes.

Furthermore, further research will allow for determining specific porosity parameters, and consequently, defining the optimal geometric characteristics of porous structures conducive to cell colonization.

CONCLUSIONS

Polyamide powders are primarily used in SLS technology for 3D printing. At this stage of research, the authors have been working exclusively with PA2200 polyamide, but are planning to conduct similar studies and tests on other materials.

PA2200 is characterized by excellent mechanical, chemical, and thermal properties, making it an ideal choice for a wide range of applications, from prototyping to the production of final parts. Additionally, this material was chosen for its biocompatibility after processing, a feature not commonly found in other materials used in this technology. The manufacturing technology that utilizes the sintering of PA2200 powders with a laser beam offers new possibilities in the field of tissue engineering substrate production. The ability to design and produce specific geometries of such constructs, both in terms of spatial characteristics and within a limited range of porosity, represents an unconventional solution that has been previously overlooked in this area. Controlling process parameters allows for the creation of structures characterized by spatial and surface porosity without the need to design the internal geometry of the construct.

During the conducted research, the authors focused on analyzing the impact of printing the process parameters on the properties of the final product. Future planned studies on other materials will allow understanding their specific characteristics and potential applications in SLS technology. This will enable to optimize printing processes for various polymer powders, which is crucial for expanding the range of applications for this technology. Extending the conducted research to other materials will provide comprehensive knowledge about their behavior during the SLS process, ultimately enabling to better tailor printing parameters to the specific requirements of different industrial applications. Proper process control will enable the production of semi-permeable membranes or scaffolds for tissue cultivation. This assumption of biocompatibility of the produced porous structure made from PA2200 powders using SLS technology has been confirmed based on micro- and macroscopic research and observations. Therefore, it can be stated that the applied 3D printing technology combined with the chosen material offers a wide range of possibilities for future applications in tissue engineering, both in terms of manufacturing culture substrates and entire systems for tissue cultivation.

REFERENCES

1. Bednarczyk E., Chondrocytes In Vitro Systems Allowing Study of OA, IJMS, 2022, 23(18): 10308, doi: 10.3390/ijms231810308.
2. Bednarczyk E., Sikora S., Jankowski K., Żołek-Tryznowska Z., Murawski T., Bańczerowski J., Lu Y., Senderowski C. Mathematical model of osteophyte development with the first attempt to identify a biomechanical parameter, Continuum Mech. Thermodyn.s, 2024, doi: 10.1007/s00161-023-01272-2.
3. Szymczyk-Ziółkowska P., Łabowska M.B., Detyna J., Michalak I., Gruber P. A review of fabrication polymer scaffolds for biomedical applications using additive manufacturing techniques, Biocybern. Biomed. Eng. 2022, 40(2): 624, doi: 10.1016/j.bbe.2020.01.015.
4. Raveling A.R., Theodossiou S.K., Schiele N.R. A 3D printed mechanical bioreactor for investigating mechanobiology and soft tissue mechanics, MethodsX, 2018, 5: 924, doi: 10.1016/j.mex.2018.08.001.
5. Pracon R. Grygoruk R., Kaczmarska E., Kepka C., Konka M., Dzielinska Z., Witkowski A., Demkow M. One extra plug to completely seal the left atrial appendage - procedure guided by 3D-printed model of the heart, Eur. Heart. J. 2017, 38, doi: 10.1093/eurheartj/ehx495.1934.
6. Pracon R., Grygoruk R., Konka M., Kepka C., Demkow M. Percutaneous closure of ventricular septal defect resulting from chest stab wound in an 18-year-old boy, Circulation: Cardiovascular Imaging, 2018, 11(11), doi: 10.1161/CIRCIMAGING.118.008326.
7. Khan I., Prabhakar A., Delepine C., Tsang H., Pham V., Sur M. A low-cost 3D printed microfluidic bioreactor and imaging chamber for live-organoid imaging, Biomicrofluidics, 2021,15(2), doi: 10.1063/5.0041027.
8. Achinas S., Heins J.-I., Krooneman J., Euverink G. J.W. Miniaturization and 3D Printing of Bioreactors: A Technological Mini Review, Micromachines, 2020, 11(9): 853, doi: 10.3390/mi11090853.
9. Gensler M. 3D printing of bioreactors in tissue engineering: A generalised approach, PLoS ONE, 2020, 15(11): 0242615, doi: 10.1371/journal.pone.0242615.
10. Skalski K., Makuch A., Wysocki B., Jankowski K., Święszkowski W. Structure and porosity of titanium scaffolds manufactured by selective laser melting, Inżynieria Powierzchni, 2018, 23(32), doi: 10.5604/01.3001.0011.8029.
11. Aschenbrenner D., Friedrich O., Gilbert D.F. 3D Printed lab-on-a-chip platform for chemical stimulation and parallel analysis of ion channel function, Micromachines, 2019, 10(8), doi: 10.3390/mi10080548.
12. Gyimah N., Scheler O., Rang T., Pardy T. Can 3D printing bring droplet microfluidics to every lab? A systematic review, Micromachines, 2021, 12(3), doi: 10.3390/mi12030339.
13. Wang H., Enders A., Preuss J.-A., Bahnemann J., Heisterkamp A., Torres-Mapa M.L. 3D printed microfluidic lab-on-a-chip device for fiber-based dual beam optical manipulation, Sci Rep, 2021, 11(1): 14584, doi: 10.1038/s41598-021-93205-9.
14. Seddiqi H. Inlet flow rate of perfusion bioreactors affects fluid flow dynamics, but not oxygen concentration in 3D-printed scaffolds for bone tissue engineering: Computational analysis and experimental validation, Comput. Biol. Med. 2020, 124: 103826, doi: 10.1016/j.compbiomed.2020.103826.
15. Yazdi A.A., Popma A., Wong W., Nguyen T., Pan Y., Xu J. 3D printing: an emerging tool for novel microfluidics and lab-on-a-chip applications, Microfluid Nanofluid, 2016, 20(3): 50, doi: 10.1007/s10404-016-1715-4.
16. Malashin I., Martysyuk D., Tynchenko V., Nelyub V., Borodulin A., Galinovsky A. Mechanical testing of selective-laser-sintered polyamide PA2200 Details: analysis of tensile properties via finite element method and machine learning approaches, Polymers 2024, 16(6): 737, doi: 10.3390/polym16060737.
17. Saffarzadeh M., Gillispie G.J., Brown P. Selective laser sintering (SLS) rapid protytping technology: A review of medical applications., In 53rd Annual Rocky Mountain Bioengineering Symposium, RMBS 2016 and 53rd International ISA Biomedical Sciences Instrumentation Symposium, 2016, 142.
18. Berry E. Preliminary experience with medical applications of rapid prototyping by selective laser sintering, Medical Engineering & Physics, 1997, 19(1): 90, doi: 10.1016/S1350-4533(96)00039-2.
19. Razaviye M.K., Tafti R.A., Khajehmohammadi M. An investigation on mechanical properties of PA12 parts produced by a SLS 3D printer: An experimental approach, CIRP Journal of Manufacturing Science and Technology, 2022, 38: 760, doi: 10.1016/j.cirpj.2022.06.016.
20. Pilipović A., Ilinčić P., Tujmer M., Rujnić Havstad M. Impact of part positioning along chamber Z-Axis and processing parameters in selective laser sintering on polyamide properties, *Appl. Sci. 2024*, 14(3): 976, doi: 10.3390/app14030976.
21. Matuš M. Geometric accuracy of components manufactured by SLS technology regarding the orientation of the model during 3D printing, Manufacturing Technology, 2023, 23(2): 233, doi: 10.21062/mft.2023.027.
22. Korycki A., Garnier C., Nassiet V., Sultan C.T., Chabert F. Optimization of mechanical properties and manufacturing time through experimental and statistical analysis of process parameters in selective laser sintering, Adv. Mater. Sci. Eng. 2022, 1–15, doi: 10.1155/2022/2526281.

23. Fabijański M., Garbarski J. Strength of thermoplastic starch filled with calcium carbonate, Przem. Chem. 2024, 103(3): 417, doi: 10.15199/62.2024.3.12.
24. Lopes A.C., Sampaio A.M., Pontes A.J. The influence of the energy density on dimensional, geometric, mechanical and morphological properties of SLS parts produced with single and multiple exposure types", Prog Addit Manuf, 2022, 7(4): 683, doi:10.1007/s40964-021-00254-7.
25. Zochowski P. Ballistic impact resistance of bulletproof vest inserts containing printed titanium structures, Metals, 2021, 11(2): 225, doi: 10.3390/met11020225.
26. Anwajler B., Szołomicki J., Noszczyk P., Baryś M. The potential of 3D printing in thermal insulating composite materials—experimental determination of the impact of the geometry on thermal resistance, Materials 2024, 17(5): 1202, doi: 10.3390/ma17051202.
27. Bernaczek J. Analysis of torsional strength of PA2200 material shape additively with the selective laser sintering technology, Adv. Sci. Technol. Res. J. 2023, 17(2): 12, doi: 10.12913/22998624/158838.
28. Zhu L. Design and compressive fatigue properties of irregular porous scaffolds for orthopedics fabricated using selective laser melting, ACS Biomater. Sci. Eng. 2021, 7(4): 1663, doi: 10.1021/acsbiomaterials.0c01392.
29. Du Y. Design and statistical analysis of irregular porous scaffolds for orthopedic reconstruction based on voronoi tessellation and fabricated via selective laser melting (SLM), Mater. Chem. Phys. 2020, 239: 121968, doi: 10.1016/j.matchemphys.2019.121968.
30. Fabijański M. Study of the single-screw extrusion process using polylactide. *Polymers* 2023, *15*: 3878. doi: 10.3390/polym15193878.
31. Garbarski J., Fabijański M. Strength of the thermoplastic starch/polylactide mixture, Przem. Chem. 2024, 103(4): 381, doi: 10.15199/62.2024.3.5.
32. https://store.eos.info/products/pa-2200-polyamide-12
33. Fabijański M. Properties of polyamide designed to be used in the elastic rail fasteners, Railway Problems, 2014, 58(165): 21.
34. Riza S.H., Masood S.H., Rashid R.A.R., Chandra S. Selective laser sintering in biomedical manufacturing, Metallic Biomaterials Processing and Medical Device Manufacturing, Elsevier, 2020, 193, doi: 10.1016/B978-0-08-102965-7.00006-0.
35. Rahim T.N.A.T., Abdullah A.M., Md Akil H., Mohamad D., Rajion V. The improvement of mechanical and thermal properties of polyamide 12 3D printed parts by fused deposition modelling, Express. Polym. Lett. 2017, 11(12): 963, doi: 10.3144/expresspolymlett.2017.92.
36. Krishnakumar S., Senthilvelan T. Polymer composites in dentistry and orthopedic applications-a review, Materials Today: Proceedings. 2021, 46: 9707, doi: 10.1016/j.matpr.2020.08.463.
37. Hariharan K., Sugavaneswaran M., Arumaikkannu G. Structural, mechanical and invitro study on pulsed laser deposition of hydroxyapatite on additive manufactured substrate, Proc. of the 2nd Intl. Conf. on Progress in Additive Manufacturing, 2016.
38. Hui D., Goodridge V., Scotchford C.A., Grant D.M. Laser sintering of nano-hydroxyapatite coated polyamide 12 powders, Additive Manufacturing, 2018, 22: 560, doi: 10.1016/j.addma.2018.05.045.
39. Rotella G., Del Prete A., Muzzupappa M., Umbrello D. Innovative manufacturing process of functionalized PA2200 for reduced adhesion properties, JMMP, 2020, 4(2): 36, doi:10.3390/jmmp4020036.
40. Papazoglou E.L., Karkalos N.E., Karmiris-Obratański P., Markopoulos A.P. On the modeling and simulation of SLM and SLS for metal and polymer powders: A review, Arch. Computat. Methods. Eng, 2022, 29(2): 941, doi: 10.1007/s11831-021-09601-x.
41. Gueche Y.A., Sanchez-Ballester N.M., Cailleaux S., Bataille B., Soulairol I. Selective laser sintering (SLS), a new chapter in the production of solid oral forms (SOFs) by 3D printing, Pharmaceutics, 2021, 13(8): 8, doi: 10.3390/pharmaceutics13081212.
42. Awad A., Fina F., Goyanes A., Gaisford S., Basit A.W. 3D printing: Principles and pharmaceutical applications of selective laser sintering, Int. J. Pharm. 2022, 586: 119594, doi: 10.1016/j.ijpharm.2020.119594.
43. Magrofuoco E., Flaibani M., Giomo M., Elvassore N. Cell culture distribution in a three-dimensional porous scaffold in perfusion bioreactor, Biochem. Eng. J. 2019, 146: 10, doi: 10.1016/j.bej.2019.02.023.
44. Voelcker N.H., Low S.P. Cell culture on porous silicon, Handbook of Porous Silicon, L. Canham, Red., Cham: Springer International Publishing, 2018, 728. doi: 10.1007/978-3-319-71381-6_50.